BASIC SCIENCE: OBSTETRICS

Chorioamnionitis induced by intraamniotic lipopolysaccharide resulted in an interval-dependent increase in central nervous system injury in the fetal sheep

A. W. Danilo Gavilanes, MD, PhD; Eveline Strackx, MSc; Boris W. Kramer, MD, PhD; Markus Gantert, MD; Daniël Van den Hove, PhD; Hellen Steinbusch; Yves Garnier, MD, PhD; Erwin Cornips, MD; Harry Steinbusch, PhD; Luc Zimmermann, MD, PhD; Johan Vles, MD, PhD

OBJECTIVE: We quantified the impact of chorioamnionitis on both the white and gray matter structures of the preterm ovine central nervous system (CNS).

STUDY DESIGN: The CNS was studied at 125 days of gestation, either 2 or 14 days after the intraamniotic administration of 10 mg of lipopolysaccharide (LPS) (*Escherichia coli*) or saline. Apoptotic cells and cell types were analyzed in the brain, cerebellum, and spinal cord using flow cytometry.

RESULTS: Apoptosis and microglial activation increased in all regions with prolonged exposure to LPS-induced chorioamnionitis. Astrocytes were increased in the brain and cerebellum of LPS-exposed fetuses but not in the spinal cord. Mature oligodendrocytes decreased in the cerebral and cerebellar white matter, the cerebral cortex, caudate putamen, and hippocampus 14 days after LPS. Neurons in the cerebral cortex, hippocampus, and substantia nigra were reduced 14 days after LPS.

CONCLUSION: Fetal inflammation globally but differentially affected the CNS depending on the maturational stage of the brain region.

Key words: central nervous system, chorioamnionitis, fetal inflammation, lipopolysaccharide, oligodendrocytes

Cite this article as: Gavilanes AWD, Strackx E, Kramer BW, et al. Chorioamnionitis induced by intraamniotic lipopolysaccharide resulted in an interval-dependent increase in central nervous system injury in the fetal sheep. Am J Obstet Gynecol 2009;200:437.e1-437.e8.

Chorioamnionitis (CA) and the corresponding fetal inflammatory response are both inversely related to gestational age in preterm infants,[1-3] affecting mainly the lungs and the central nervous system (CNS).[4-7] The predominantly studied CNS pathology is cerebral periventricular white matter (WM) disease (WMD), which results in permanent structural brain damage and severe long-lasting neurodevelopmental impairment, such as periventricular leukomalacia.[8,9] Cortical and subcortical gray matter (GM) and cerebellum are affected as well, contributing to a complex long-term neurologic morbidity.[10,11]

This study aimed to overcome 2 general drawbacks from the most commonly used experimental paradigms. First, lipopolysaccharide (LPS) is usually given intravenously (IV) to induce fetal inflammation. In addition to fetal inflammation, however, this approach also induces important superimposed hypoxia ischemia.[12] Second, little attention has been paid to other CNS regions besides the cerebral WM. To overcome the first drawback, we studied the sheep CNS pathology after CA by LPS administration into the amniotic fluid. This intraamniotic administration avoids the hemodynamic changes and the secondary postasphyctic encephalopathy induced by fetal IV LPS.[13,14] In addition, this experimental time window corresponds to approximately 28 weeks of human CNS maturation, which is the most vulnerable period for the human brain to develop WMD.[15-17] To overcome the second drawback, we studied the regional impact on the developing CNS in different regions of the WM and GM using flow cytometry. We hypothesize both a global CNS impact and a time-related effect after LPS-induced CA.

From the Departments of Pediatrics–Neonatology (Drs Gavilanes, Kramer, and Zimmermann and Ms Strackx), Child Neurology (Ms Strackx and Dr Vles), and Neurosurgery (Dr Cornips), University Hospital Maastricht, in collaboration with the Research Institute of Growth and Development (GROW), Maastricht, The Netherlands; the Faculty of Health, Medicine and Life Sciences, School of Mental Health and Neuroscience, Maastricht University, and European Graduate School of Neuroscience (EURON), Maastricht, The Netherlands (Dr Van den Hove, and Ms Hellen Steinbusch, Mr Harry Steinbusch, and Ms Strackx); and the Department of Obstetrics and Gynecology, University of Köln, Köln, Germany (Drs Gantert and Garnier).

Received May 26, 2008; revised July 20, 2008; accepted Dec. 4, 2008.

Reprints: A. W. Danilo Gavilanes, MD, Department of Pediatrics, Division of Neonatology, Maastricht University Medical Center, PO Box 5800, NL-6200 AZ Maastricht, The Netherlands. danilo.gavilanes@mumc.nl.

The first 2 authors contributed equally to this research.

 • doi: 10.1016/j.ajog.2008.12.003

MATERIALS AND METHODS

Animals and surgical procedures

All experimental procedures were approved by our animal ethics board accord-

FIGURE 1
Body and brain weights

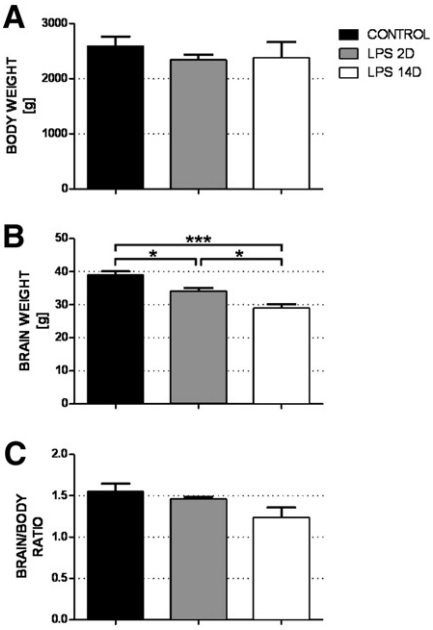

Effect of fetal endotoxin exposure on body and brain weight. **A,** No significant differences in bodyweight between groups. **B**, Brain weight was significantly lower in lipopolysaccharide (LPS) 2-day (2D) and 14-day (14D) groups than in control group. **C,** Endotoxin exposure did not cause any changes in brain to body ratio among 3 groups. Data are represented as mean + SEM. *Black bars* = control (n = 7); *gray bars* = LPS 2D (n = 5); and *white bars* = LPS 14D (n = 6) groups. Multivariate analysis of variance + Bonferroni testing; $*P < .05$ and $***P < .001$.

Gavilanes. CA induced by intraamniotic LPS resulted in an interval-dependent increase in CNS injury in the fetal sheep. Am J Obstet Gynecol 2009.

ing to Dutch government regulations. Pregnant Texel ewes, bearing both singletons and twins, were housed outdoors. Food and water were provided ad libitum. LPS (10 mg dissolved in 2 mL sterile and filtered saline) was injected intraamniotically (IA) under ultrasound guidance at day 123 of gestation (n = 5) or at day 111 of gestation (n = 6). Control saline injection was given at either day 111 or 123 of gestation (n = 7).[18] At day 125 of gestation, pregnant ewes were anesthetized and all fetuses were delivered by cesarean section. Fetuses were killed by a lethal injection of pentobarbital. The brain was removed and halved. One half was prepared for flow cytometric analysis.

Tissue preparation

The cerebral cortex, caudate nucleus and putamen (CPU), hippocampus, frontal periventricular WM, hypothalamus, substantia nigra (SN), C1, T11, and L1 of the spinal cord (SC), and cerebellar cortex and WM were dissected and placed in ice-cold plating medium consisting of Dulbecco's Modified Eagle's medium supplemented with 10% fetal bovine serum (FBS), penicillin/streptavidin, and glutamate. The tissue was mechanically disrupted using a glass homogenizer. The suspension was centrifuged at 1200 rpm at 4°C for 10 minutes, and the pellet was resuspended in 5 mL of plating medium. The crude cell suspension was then passed through a 100-μm nylon cell strainer to remove large cell clumps. The cells were counted using a cell counting chamber and divided into different microcentrifuge tubes (10^6 cells/0.5 mL/tube). The viability of the cells was monitored using trypan blue staining.

Flow cytometric analysis

AnnexinV/propidium iodide staining

Apoptotic and necrotic cells were detected with annexinV conjugated to fluorescin (FITC) and propidium iodide (PI) (AnnexinV-FITC Apoptosis Detection Kit; BD Biosciences Pharmingen, Breda, The Netherlands). The cells were washed twice with phosphate buffered saline (PBS), followed by a wash in AnnexinV-binding buffer. Then, all samples (10^7 cells/100 μL) were incubated with 5 μL of AnnexinV antibody and 5 μL of PI for 15 minutes at room temperature (RT).

Extracellular staining (OX42)

OX42 was used to identify activated microglia. The cells were washed twice with staining buffer (PBS + 2% FBS) by centrifugation at 1200 rpm at 4°C and incubated for 30 minutes at RT with the primary antibody: mouse antibovine CD11b/c (clone OX42; AbD Serotec, Huissen, The Netherlands), diluted 1:100 in staining buffer. The cells were washed twice followed by incubation with the secondary antibody: donkey antimouse alexa 488 diluted 1:100 in staining buffer. All samples were washed and kept at 4°C in the dark.

Intracellular staining (glial fibrillary acidic protein, 2′,3′-cyclic nucleotide 3′-phosphodiesterase, and antineurofilament 200-kd)

Antiglial fibrillary acidic protein antibodies were used to identify activated astrocytes. Anti-2′,3′-cyclic nucleotide 3′-phosphodiesterase antibodies were used to detect mature oligodendrocytes, whereas antineurofilament 200-kd antibodies were used to detect neurons. Cells were washed twice with staining buffer by centrifugation at 1200 rpm at 4°C. After washing, cells were fixed with 4% paraformaldehyde in staining buffer (2% final concentration) for 20 minutes at RT. Permeabilization was done after 2 more washing steps with permeabilization buffer (0.05% saponin + 2% FBS + PBS) for 10 minutes at RT. The cell suspension was then incubated with the primary antibody for 30 or 45 minutes at RT. The antibodies were mouse antiovine 2′,3′-cyclic nucleotide phosphodiesterase (clone 11-5B; Sigma, Munich, Germany); monoclonal antibody 1:200 in permeabilization buffer/rabbit antiovine glial fibrillary acidic protein (Dako, Glostrup, Denmark); and polyclonal antibody 1:200 in permeabilization buffer/mouse antineurofilament 200-kd (Abcam, Cambridge, UK); and monoclonal antibody 1:100 in permeabilization buffer. After 2 washing steps, the cell suspension was incubated with the secondary antibody (respectively donkey antimouse or donkey antirabbit alexa 488 diluted 1:100 in permeabilization buffer) again for 30 minutes at RT. All samples were washed 2 times and kept at 4°C in the dark.

Flow cytometry

All samples were run on an FACScalibur flow cytometry system (BD Biosciences, San Jose, CA), equipped with an argon ion laser (488 nm). Analysis was done using the Cell Quest Pro software (BD Biosciences). Forward and sideward light angle scatters were collected from all samples. Using those plots, samples were gated (region 1; R1) to exclude cell debris and cellular aggregates for further analysis. For each marker, the mean fluorescence intensity and the percentage of positive cells stained above background were measured for a total of 10,000 cells per sample within the gate (R1). The cut-

FIGURE 2
Flow cytograms

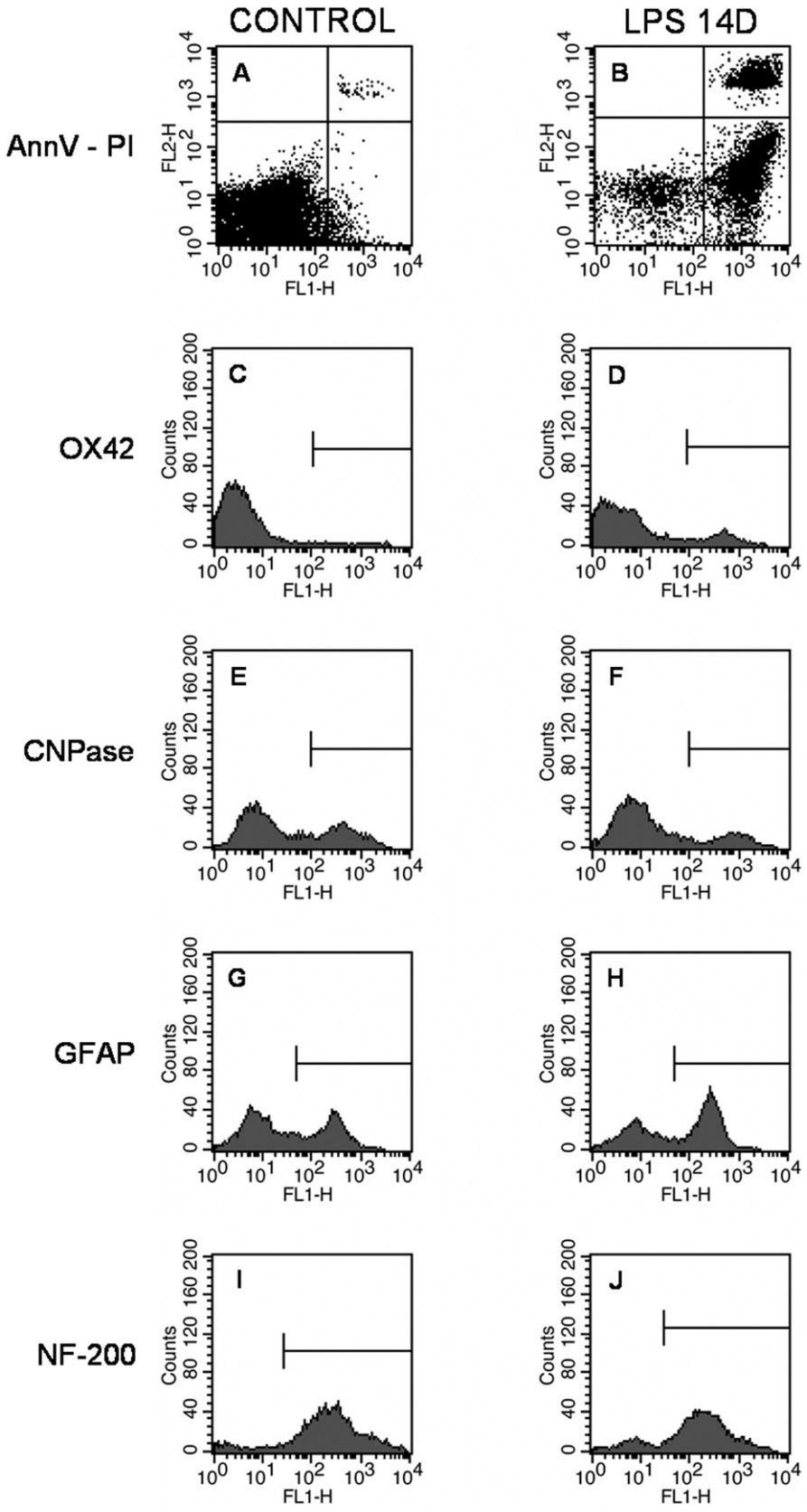

off was defined using control tissue negative for the different markers processed and stained alongside the experimental samples. The mean fluorescence intensity was corrected for autofluorescence using the values from cells only incubated with secondary antibody.

Statistical analysis

Data were analyzed using a multivariate analysis of variance (mean ± SEM). Significant effects were analyzed by post hoc Bonferroni corrections. The accepted level of significance was $P < .05$. All calculations were done using software (SPSS 12.0; SPSS, Inc, Chicago, IL).

Representative flow cytograms of control and lipopolysaccharide (LPS) 14-day (14D) animals. Flow cytograms of AnnexinV (AnnV) binding vs propidium iodide (PI) uptake of **A**, control and **B**, LPS 14D animals. Four populations of cells are visualized. Viable cells, in *lower left quadrant* (Q3), are double negative. Apoptotic cells in *lower right quadrant* (Q4) are $AnnV^+$ and PI^-. Double-positive cells ($AnnV^+/PI^+$) are in *upper right quadrant* (Q2). They are thought to be necrotic or advanced apoptotic. Cells in *last quadrant* (*upper left*, Q1) are isolated nuclei or cellular debris. There was significant decrease in number of viable cells in LPS 14D animal as compared with control animal. Further, significant increase in apoptotic (Q4) and necrotic index (Q2) was observed in LPS 14D animal compared with control animal. Flow cytograms of **C** and **D**, OX42, **E** and **F**, 2′,3′-cyclic nucleotide 3′-phosphodiesterase (CNPase), **G** and **H** glial fibrillary acidic protein (GFAP), and **I** and **J**, antineurofilament 200-kd (NF-200) staining of **C**, **E**, **G**, and **I**, control and **D**, **F**, **H**, and **J**, LPS 14D animals. Data were plotted as fluorescence (FL_1) in function of number of counts. Percentage of positive cells in histograms is indicated by line. There was significant increase in percentage of activated microglia and astrocytes in LPS 14D compared with control animal. Moreover, proportion of mature oligodendrocytes and neurons was lower in LPS 14D animal than in control animal.

Gavilanes. CA induced by intraamniotic LPS resulted in an interval-dependent increase in CNS injury in the fetal sheep. Am J Obstet Gynecol 2009.

FIGURE 3
Apoptosis and necrosis

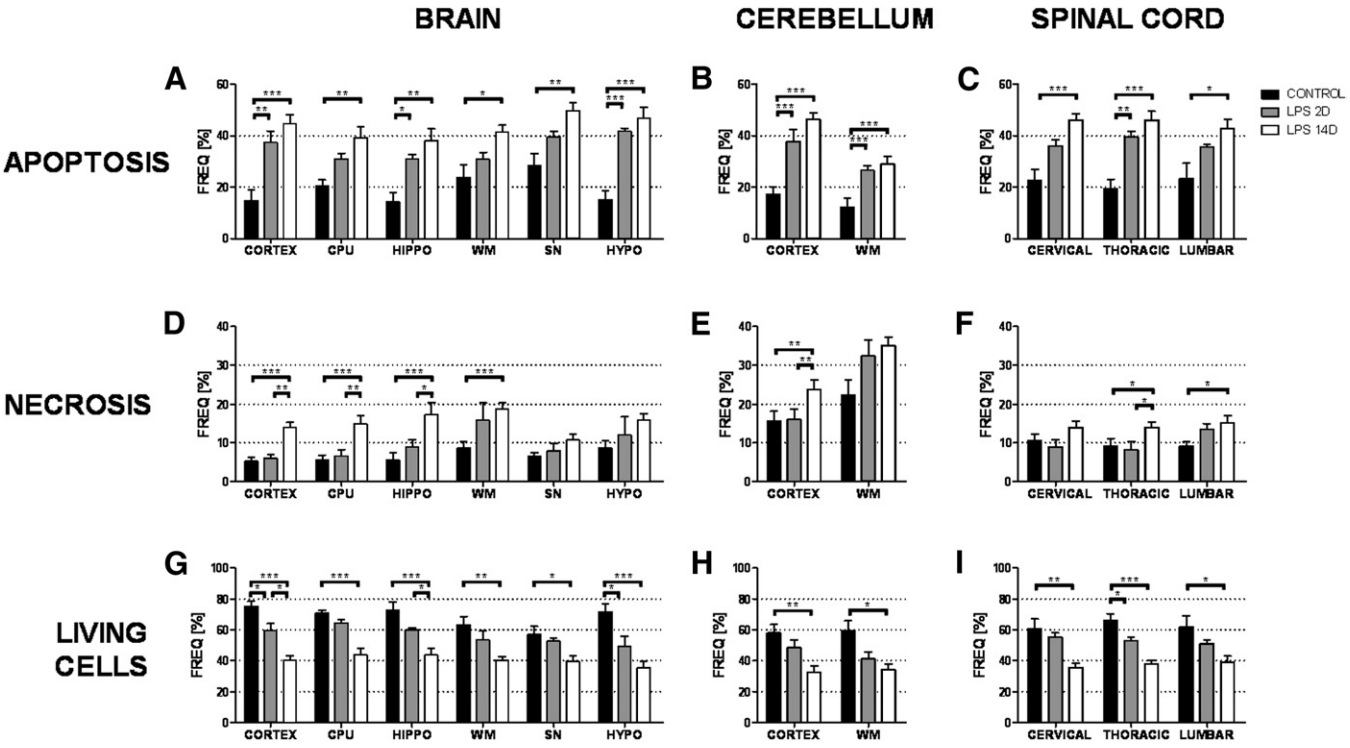

Differences in percentage of apoptotic, necrotic, and living cells in brain, cerebellum, and spinal cord. Percentage of apoptotic cells in **A**, brain, **B**, cerebellum, and **C**, spinal cord. Percentage of necrotic cells in **D**, brain, **E**, cerebellum, and **F**, spinal cord. Percentage of living cells in **G**, brain, **H**, cerebellum, and **I**, spinal cord. Data are represented as mean percentage of positive cells + SEM. *Black bars* = control (n = 7); *gray bars* = lipopolysaccharide (LPS) 2-day (n = 5); and *white bars* = LPS 14-day (n = 6) groups. Multivariate analysis of variance + Bonferroni testing; $*P < .05$, $**P < .01$, and $***P < .001$.

CPU, caudate putamen; *HIPPO*, hippocampus; *hypo*, hypothalamus; *SN*, substantia nigra; *WM*, white matter.
Gavilanes. CA induced by intraamniotic LPS resulted in an interval-dependent increase in CNS injury in the fetal sheep. Am J Obstet Gynecol 2009.

RESULTS

Brain and bodyweight

The mean body and brain weights of the LPS 2-day (n = 5), LPS 14-day (n = 6), and control (n = 7) groups are shown in Figure 1. There were no significant differences in body weight among the 3 groups (Figure 1, A). The mean brain weight of both the LPS 2-day ($P = .031$) and LPS 14-day ($P < .001$) group was significantly lower than the mean brain weight of the control group (Figure 1, B). A significant difference between the LPS 2-day and the LPS 14-day group was shown, with the last group being most affected ($P = .048$ vs control). The percentage brain of total body weight did not differ significantly between the different groups (Figure 1, C).

Apoptotic and necrotic cell death

Figure 2, A and B, shows representative examples of the histograms of a control animal and LPS 14-day animal. Percentages of living (AnnexinV$^-$ and PI$^-$), apoptotic (AnnexinV$^+$ and PI$^-$), and necrotic (AnnexinV$^+$ and PI$^+$) cells are given in Figure 3. Double-negative (AnnexinV$^-$/PI$^-$) cells are viable cells (Figure 3, G-I). Values of living cells were significantly lower in the LPS 14-day group (33-43%) in all CNS areas investigated compared with controls (57-75%). Only the cortex, hippocampus, hypothalamus, and the T11 level of the SC showed a significant decrease in the LPS 2-day group. AnnexinV$^+$/PI$^-$ cells are considered to be apoptotic cells (Figure 3, A-C). The percentage of apoptotic cells increased significantly in the LPS 14-day group (28-46%) compared with the saline group (12-23%) in all regions of interest. In the cortex, hippocampus, hypothalamus, cerebellar cortex, cerebellar WM, and T11 level of the SC, the percentage of apoptotic cells in the LPS 2-day group was higher than in controls. Double-positive cells (AnnexinV$^+$/PI$^+$) are considered to undergo necrosis or advanced apoptosis (Figure 3, D-F). A significant increase in the necrotic index in the LPS 14-day group (14-30%) in comparison with the saline group (5-22%) was shown in the cerebral cortex, CPU, hippocampus and periventricular WM in the brain, T11 and L1 level of SC, and in the cerebellar WM. In addition, there was also a significant increase in the necrotic in-

FIGURE 4
CNS cell populations

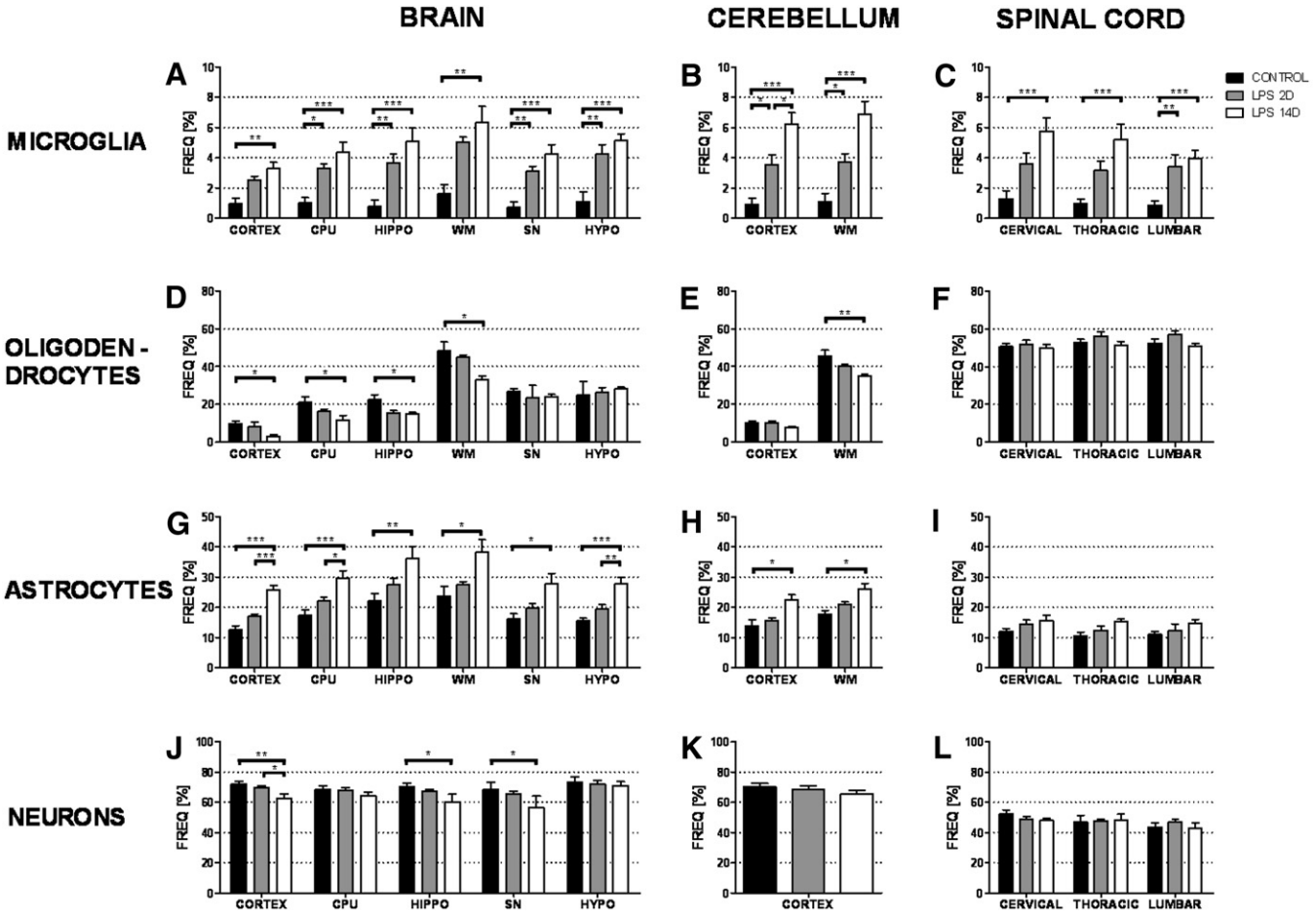

Differences in percentage of microglia, oligodendrocytes, astrocytes, and neurons in brain, spinal cord, and cerebellum. Percentage of microglia in **A**, brain, **B**, cerebellum, and **C**, spinal cord. Percentage of oligodendrocytes in **D**, brain, **E**, cerebellum, and **F**, spinal cord. Percentage of astrocytes in **G**, brain, **H**, cerebellum, and **I**, spinal cord. Percentage of neurons in **J**, brain, **K**, cerebellum, and **L**, spinal cord. Data are represented as mean percentage of positive cells + SEM. *Black bars* = control (n = 7); *gray bars* = lipopolysaccharide (LPS) 2-day (n = 5); and *white bars* = LPS 14-day (n = 6) groups. Multivariate analysis of variance + Bonferroni testing; $*P < .05$, $**P < .01$, and $***P < .001$.

CNS, central nervous systems; *CPU*, caudate putamen; *HIPPO*, hippocampus; *hypo*, hypothalamus; *SN*, substantia nigra; *WM*, white matter.
Gavilanes. CA induced by intraamniotic LPS resulted in an interval-dependent increase in CNS injury in the fetal sheep. Am J Obstet Gynecol 2009.

dex in the cortex, CPU, hippocampus, T11 level of the SC, and cerebellar cortex in the LPS 14-day group compared with the LPS 2-day group. The necrotic index was not different in the SN, hypothalamus, C1 of the SC, or the cerebellar cortex.

Cell populations

Activated microglia

The representative histograms are shown in Figure 2, C and D. The number of activated microglia ($OX42^+$) was very low in the saline group (0.8-1.6%). In almost all regions (CPU, hippocampus, SN, hypothalamus, L1 level of SC, the cerebellar cortex, and cerebellar WM), the percentage of activated microglia was significantly higher in the LPS 2-day group (2.5-5%) than in the saline group. There was an even higher increase in the proportion of activated microglia in the LPS 14-day group (3.2-6.8%), affecting all areas investigated (Figure 4, A-C).

Mature oligodendrocytes

The representative histograms are shown in Figure 2, E and F. The values of the mature oligodendrocytes observed were similar for the saline (9-52%) and the LPS 2-day (8-57%) groups for all areas investigated (Figure 4, D-F). In the cortex, CPU, hippocampus, periventricular WM, and cerebellar WM, the proportion of mature oligodendrocytes was much lower in the LPS 14-day group (3-35%) than in the saline group (9-45%). All other regions investigated were not affected in the LPS 14-day group.

Reactive astrocytes

The representative plots are shown in Figure 2, G and H. No significant differences were found in the percentage of astrocytes in the LPS 2-day group (12-27%) compared with the saline group (10-22%) (Figure 4, G-I). However, in the LPS 14-day group (14-36%) a

significant increase in the proportion of astrocytes was observed in all areas of the brain and cerebellum. The SC, in contrast, was not affected.

Neurons

No significant differences were found in the proportion of neurons between the control (41-82%) and the LPS 2-day (43-82%) groups for any of the areas investigated (Figure 4, J-L); representative histogram is in Figure 2, I and J. In the LPS 14-day group (41-73%), however, the percentages of neurons were significantly lower in the cortex, hippocampus, and SN compared with the control group. No differences were detected in the cerebellum or SC.

There was no influence of sex, singleton/twin, or weight on any of the analyzed variables.

COMMENT

CA resulted in an interval-dependent increase in CNS injury and different regional injury patterns. Microglial activation and apoptotic cell death were increased in all brain, cerebellum, and SC regions in an interval-dependent manner. In addition, most brain regions showed reductions in oligodendrocytes and neurons and an increase in astrocytes, whereas the cerebellum and especially the SC seemed to be less affected. This study is the first to show a global inflammatory response to acute CA in the brain, cerebellum, and SC and a selective vulnerability of the developing regions.

These changes might be explained by the state of CNS maturation at that given gestational age. In the fetal brain, the WM is predominantly affected by systemic inflammation/infection as highlighted by fetal animal experiments in rabbits, guinea pigs, mice, rats, and sheep.[19-24] Furthermore, CA is associated with both cerebral palsy and WMD seen with neonatal imaging.[5,7,25] More recent evidence points toward a relationship between WMD and GM abnormalities.[11] This could explain the permanent neurodevelopmental and intellectual deficits in ex-preterm infants, which are not limited to cerebral palsy.[26] The use of this model of CA has several advantages, making it clinically more relevant than others. First, the CA-associated systemic inflammation has been previously characterized in this model by Kramer et al.[13] Second, the IA LPS strategy avoids the superimposed hypoxia ischemia of the IV strategy and the local processes caused by an intracerebral route.[12,27] Third, species with a long gestation duration, such as human beings and sheep, share several aspects of development and function. In addition, the current study not only focused on brain WMD, but it also analyzed the effect of developmental inflammation on both the cerebral cortical and subcortical GM structures and the cerebellar and SC regions. Experimental data combining all these regions are not available.

The loss of oligodendrocytes, especially in the periventricular and the subcortical WM, has been reported before in intracerebral, IV, intrauterine, and maternal LPS models in different animal species.[27-31] In addition, a previous study using a similar ovine intraamniotic LPS model also demonstrated a decrease in oligodendrocytes in the areas of extensive focal damage.[20] In contrast to our study, no global effects were previously found on the density and/or number of mature oligodendrocytes throughout the whole brain. Moreover, our study showed a decreased number of neurons in the cortex, hippocampus, and SN in the LPS 14-day group compared with the control group, whereas neither the cerebellum nor the SC differed from the control animals. GM and/or neuron-specific damage have not been identified before in intracerebral or IV LPS models.[31] Maternal administration of LPS in rats, however, led to a loss of tyrosine hydroxylase-positive neurons in the SN of 16-month-old offspring.[32] In addition, maternal LPS caused the loss of pyramidal cells in the hippocampus at the age of 8 months.[33]

Apoptotic cell death was increased in some of the regions in the LPS 2-day group (cortex, hippocampus, hypothalamus, cerebellar cortex, cerebellar WM, and T11) and in all areas studied in the LPS 14-day group. Necrotic cells were also higher in most areas of the LPS 14-day group compared with the control group (cortex, CPU, hippocampus, periventricular WM, and cerebellar cortex T11 and L1). In a human postmortem study, apoptosis has already been reported as a contributing mechanism for cell death in infants with WMD.[34] Garnier et al[35] also found evidence of apoptotic cell death, especially in the periventricular WM, in a sheep model for IV LPS. Moreover, an intracervical LPS injection of pregnant rats led to the activation of both the intrinsic and the extrinsic pathway of apoptosis.[36] One possible explanation for LPS-induced apoptotic cell death could be that LPS causes the up-regulation of the systemic production of tumor necrosis factor (TNF)-α, activating the TNF-α-caspase pathway and an increased production by microglia and astrocytes in the brain.[13,37,38] Apoptosis has been reported to affect mainly oligodendrocytes and/or their precursors,[34,39] but our study suggests that neurons are affected as well.

Microglial activation was increased in all regions of both LPS groups with the exception of cerebral cortex and WM, and the C1 and T11 level of SC in the LPS 2-day group. Increased astrocytic activation was observed in all areas of the brain and cerebellum in the LPS 14-day group, whereas the SC was not affected. Similar increases were found in almost all other LPS models, in particular in the cerebral WM.[27,29-31] Our study shows for the first time general microglial activation or astrogliosis throughout the whole brain. The activation of microglia and astrocytes in the brain may be caused by the entry of systemic inflammatory cells and cytokines through a permeable blood-brain barrier. Activated microglia and astrocytes respond to an inflammatory insult, which may affect the WM and, second, explain the concomitant selective GM compromise. First, neurons destined for the frontal cerebral cortex migrate through the developing WM and form the subplate during late gestation.[40] These subplate neurons are the only neuronal element of developing cerebral WM and persist up to 6 months postnatally.[26] They may guide thalamocortical and cortical axons.[26,41] In patients with WMD, apoptotic changes are seen in subplate neurons, WM, and cor-

tex.[40] Second, oligodendroglial-axonal interactions are critical for axonal and neuronal development. Therefore, the injury to preoligodendrocytes in WMD could contribute neuronal disruption.[26] This GM compromise has been recently shown by quantitative volumetric magnetic resonance imaging analysis in ex-preterm infants, where WMD was associated with both a reduced cerebral cortical and basal ganglia volume and with a reduced thalamic volume.[42-44] In addition, WM and cortical GM volume reductions are correlated with working memory deficits at 2 years of corrected age and hippocampal volume reductions are correlated with a memory impairment in ex-preterm infants at 13 years.[45,46] Further, qualitative term magnetic resonance imaging analysis with WMD is positively correlated with superimposed GM abnormalities and global deficits at 2 years of corrected age in ex-preterm infants.[47]

Myelination proceeds from caudal in the first trimester of gestation to rostral up until infancy.[48] This maturational hierarchy is a plausible explanation for the lesser general impact of CA on the SC as compared with the cerebellum and brain, and the unchanged cerebellar neuronal counts in LPS-treated animals. The developing cerebellum is of particular importance because it might not only influence motor control and posture, but also the more complex cognitive processes.[49,50]

In summary, the CNS inflammatory impact was universal, because all subjects of a given group were almost equally affected. The impact was also interval dependent, because damage was more prominent in the 14-day CA group than in the 2-day group. Moreover, the impact showed selective regional differences, meaning that neither astrocytic and neuronal SC changes nor neuronal cerebellar changes were found in either CA group. Whether the differences between groups are caused by: (1) length of intraamniotic LPS exposure (2- vs 14-day interval); (2) stage of fetal neurodevelopment at the time of LPS exposure (day 111 of gestation vs day 123 of gestation); or (3) both cannot be differentiated on the basis of the experimental design of this study.

These findings are relevant because this is the first study showing both global WM and GM impact of an acute CA in association with regional differences. ■

ACKNOWLEDGMENTS

We thank Dr Vincent Roelfsema and Dr Odette Besancon for their collaboration and the animal laboratory team for their assistance during the experiments. Our special thanks to Prof Marc De Baets for the generous facilitation of the flow cytometry equipment.

REFERENCES

1. Lahra MM, Jeffery HE. A fetal response to chorioamnionitis is associated with early survival after preterm birth. Am J Obstet Gynecol 2004;190:147-51.

2. Pacora P, Chaiworapongsa T, Maymon E, et al. Funisitis and chorionic vasculitis: the histological counterpart of the fetal inflammatory response syndrome. J Matern Fetal Neonatal Med 2002;11:18-25.

3. Yoon BH, Romero R, Park JS, et al. The relationship among inflammatory lesions of the umbilical cord (funisitis), umbilical cord plasma interleukin 6 concentration, amniotic fluid infection, and neonatal sepsis. Am J Obstet Gynecol 2000;183:1124-9.

4. Dammann O, Leviton A, Bartels DB, Dammann CE. Lung and brain damage in preterm newborns. Are they related? How? Why? Biol Neonate 2004;85:305-13.

5. Wu YW. Systematic review of chorioamnionitis and cerebral palsy. Ment Retard Dev Disabil Res Rev 2002;8:25-9.

6. Wu YW, Escobar GJ, Grether JK, Croen LA, Greene JD, Newman TB. Chorioamnionitis and cerebral palsy in term and near-term infants. JAMA 2003;290:2677-84.

7. Yoon BH, Romero R, Park JS, et al. Fetal exposure to an intra-amniotic inflammation and the development of cerebral palsy at the age of three years. Am J Obstet Gynecol 2000;182:675-81.

8. Back SA, Riddle A, McClure MM. Maturation-dependent vulnerability of perinatal white matter in premature birth. Stroke 2007;38:724-30.

9. Leviton A, Paneth N, Reuss ML, et al. Maternal infection, fetal inflammatory response, and brain damage in very low birth weight infants: developmental epidemiology network investigators. Pediatr Res 1999;46:566-75.

10. Shah DK, Anderson PJ, Carlin JB, et al. Reduction in cerebellar volumes in preterm infants: relationship to white matter injury and neurodevelopment at two years of age. Pediatr Res 2006;60:97-102.

11. Thompson DK, Warfield SK, Carlin JB, et al. Perinatal risk factors altering regional brain structure in the preterm infant. Brain 2007;130:667-77.

12. Garnier Y, Coumans A, Berger R, Jensen A, Hasaart TH. Endotoxemia severely affects circulation during normoxia and asphyxia in immature fetal sheep. J Soc Gynecol Investig 2001;8:134-42.

13. Kramer BW, Moss TJ, Willet KE, et al. Dose and time response after intraamniotic endotoxin in preterm lambs. Am J Respir Crit Care Med 2001;164:982-8.

14. Nitsos I, Moss TJ, Cock ML, Harding R, Newnham JP. Fetal responses to intra-amniotic endotoxin in sheep. J Soc Gynecol Investig 2002;9:80-5.

15. Back SA. Recent advances in human perinatal white matter injury. Prog Brain Res 2001;132:131-47.

16. Back SA, Riddle A, Hohimer AR. Role of instrumented fetal sheep preparations in defining the pathogenesis of human periventricular white-matter injury. J Child Neurol 2006;21:582-9.

17. Duncan JR, Cock ML, Scheerlinck JP, et al. White matter injury after repeated endotoxin exposure in the preterm ovine fetus. Pediatr Res 2002;52:941-9.

18. Jobe AH, Newnham JP, Willet KE, et al. Effects of antenatal endotoxin and glucocorticoids on the lungs of preterm lambs. Am J Obstet Gynecol 2000;182:401-8.

19. Elovitz MA, Mrinalini C, Sammel MD. Elucidating the early signal transduction pathways leading to fetal brain injury in preterm birth. Pediatr Res 2006;59:50-5.

20. Nitsos I, Rees SM, Duncan J, et al. Chronic exposure to intra-amniotic lipopolysaccharide affects the ovine fetal brain. J Soc Gynecol Investig 2006;13:239-47.

21. Patrick LA, Gaudet LM, Farley AE, Rossiter JP, Tomalty LL, Smith GN. Development of a guinea pig model of chorioamnionitis and fetal brain injury. Am J Obstet Gynecol 2004;191:1205-11.

22. Poggi SH, Park J, Toso L, et al. No phenotype associated with established lipopolysaccharide model for cerebral palsy. Am J Obstet Gynecol 2005;192:727-33.

23. Ramsey PS, Lieman JM, Brumfield CG, Carlo W. Chorioamnionitis increases neonatal morbidity in pregnancies complicated by preterm premature rupture of membranes. Am J Obstet Gynecol 2005;192:1162-6.

24. Yoon BH, Kim CJ, Romero R, et al. Experimentally induced intrauterine infection causes fetal brain white matter lesions in rabbits. Am J Obstet Gynecol 1997;177:797-802.

25. Yoon BH, Romero R, Yang SH, et al. Interleukin-6 concentrations in umbilical cord plasma are elevated in neonates with white matter lesions associated with periventricular leukomalacia. Am J Obstet Gynecol 1996;174:1433-40.

26. Volpe JJ. Encephalopathy of prematurity includes neuronal abnormalities. Pediatrics 2005;116:221-5.

27. Pang Y, Cai Z, Rhodes PG. Disturbance of oligodendrocyte development, hypomyelination and white matter injury in the neonatal rat brain after intracerebral injection of lipopolysaccharide. Brain Res Dev Brain Res 2003;140:205-14.
28. Lehnardt S, Lachance C, Patrizi S, et al. The toll-like receptor TLR4 is necessary for lipopolysaccharide-induced oligodendrocyte injury in the CNS. J Neurosci 2002;22:2478-86.
29. Mallard C, Welin AK, Peebles D, Hagberg H, Kjellmer I. White matter injury following systemic endotoxemia or asphyxia in the fetal sheep. Neurochem Res 2003;28:215-23.
30. Paintlia MK, Paintlia AS, Barbosa E, Singh I, Singh AK. N-acetylcysteine prevents endotoxin-induced degeneration of oligodendrocyte progenitors and hypomyelination in developing rat brain. J Neurosci Res 2004;78:347-61.
31. Wang X, Rousset CI, Hagberg H, Mallard C. Lipopolysaccharide-induced inflammation and perinatal brain injury. Semin Fetal Neonatal Med 2006;11:343-53.
32. Ling Z, Chang QA, Tong CW, Leurgans SE, Lipton JW, Carvey PM. Rotenone potentiates dopamine neuron loss in animals exposed to lipopolysaccharide prenatally. Exp Neurol 2004;190:373-83.
33. Golan HM, Lev V, Hallak M, Sorokin Y, Huleihel M. Specific neurodevelopmental damage in mice offspring following maternal inflammation during pregnancy. Neuropharmacology 2005;48:903-17.
34. Chamnanvanakij S, Margraf LR, Burns D, Perlman JM. Apoptosis and white matter injury in preterm infants. Pediatr Dev Pathol 2002;5:184-9.
35. Garnier Y, Berger R, Alm S, et al. Systemic endotoxin administration results in increased S100B protein blood levels and periventricular brain white matter injury in the preterm fetal sheep. Eur J Obstet Gynecol Reprod Biol 2006;124:15-22.
36. Sharangpani A, Takanohashi A, Bell MJ. Caspase activation in fetal rat brain following experimental intrauterine inflammation. Brain Res 2008;1200:138-45.
37. Cammer W. Effects of TNFalpha on immature and mature oligodendrocytes and their progenitors in vitro. Brain Res 2000;864:213-9.
38. Eklind S, Hagberg H, Wang X, et al. Effect of lipopolysaccharide on global gene expression in the immature rat brain. Pediatr Res 2006;60:161-8.
39. Bell MJ, Hallenbeck JM. Effects of intrauterine inflammation on developing rat brain. J Neurosci Res 2002;70:570-9.
40. Robinson S, Li Q, Dechant A, Cohen ML. Neonatal loss of gamma-aminobutyric acid pathway expression after human perinatal brain injury. J Neurosurg 2006;104:396-408.
41. Kostovic I, Jovanov-Milosevic N. The development of cerebral connections during the first 20-45 weeks' gestation. Semin Fetal Neonatal Med 2006;11:415-22.
42. Inder TE, Warfield SK, Wang H, Huppi PS, Volpe JJ. Abnormal cerebral structure is present at term in premature infants. Pediatrics 2005;115:286-94.
43. Lin Y, Okumura A, Hayakawa F, Kato K, Kuno T, Watanabe K. Quantitative evaluation of thalami and basal ganglia in infants with periventricular leukomalacia. Dev Med Child Neurol 2001;43:481-5.
44. Srinivasan L, Dutta R, Counsell SJ, et al. Quantification of deep gray matter in preterm infants at term-equivalent age using manual volumetry of 3-tesla magnetic resonance images. Pediatrics 2007;119:759-65.
45. Gimenez M, Junque C, Narberhaus A, et al. Hippocampal gray matter reduction associates with memory deficits in adolescents with history of prematurity. Neuroimage 2004;23:869-77.
46. Woodward LJ, Edgin JO, Thompson D, Inder TE. Object working memory deficits predicted by early brain injury and development in the preterm infant. Brain 2005;128:2578-87.
47. Woodward LJ, Anderson PJ, Austin NC, Howard K, Inder TE. Neonatal MRI to predict neurodevelopmental outcomes in preterm infants. N Engl J Med 2006;355:685-94.
48. Holland BA, Haas DK, Norman D, Brant-Zawadzki M, Newton TH. MRI of normal brain maturation. AJNR Am J Neuroradiol 1986;7:201-8.
49. Hutton LC, Castillo-Melendez M, Walker DW. Uteroplacental inflammation results in blood brain barrier breakdown, increased activated caspase 3 and lipid peroxidation in the late gestation ovine fetal cerebellum. Dev Neurosci 2007;29:341-54.
50. Hutton LC, Yan E, Yawno T, Castillo-Melendez M, Hirst JJ, Walker DW. Injury of the developing cerebellum: a brief review of the effects of endotoxin and asphyxial challenges in the late gestation sheep fetus. Cerebellum 2007;3:1-10.